Nuclear Overhauser Enhancement Spectroscopy Cross-Relaxation Rates and Ethanol Distribution across Membranes

Scott E. Feller,* Christopher A. Brown,* David T. Nizza,† and Klaus Gawrisch†

*Department of Chemistry, Wabash College, Crawfordsville Indiana 47933 USA; and †Laboratory of Membrane Biochemistry and Biophysics, NIAAA, National Institutes of Health, Rockville, Maryland 20852 USA

ABSTRACT Measurement of nuclear Overhauser enhancement spectroscopy cross-relaxation rates between ethanol and palmitoyloleoylphosphatidylcholine bilayers was combined with atomic-level molecular dynamics simulations. The molecular dynamics trajectories yielded autocorrelation functions of proton dipole-dipole interactions, and, consequently, relaxation times and cross-relaxation rates. These analyses allow the measured cross-relaxation rates to be interpreted in terms of relative interaction strengths with the various segments of the lipid molecule. We determined that cross-relaxation between ethanol and specific lipid resonances is primarily determined by the sites of interaction with some modulation due to lipid disorder and to local differences in intramolecular lipid dynamics. The rates scale linearly with the lifetime of temporary ethanol-lipid associations. Ethanol interacts with palmitoyloleoylphosphatidylcholine bilayers primarily via hydrophilic interactions, in particular the formation of hydrogen bonds to the lipid phosphate group. There is a weak contribution to binding from hydrophobic interaction with lipid chain segments near the glycerol. However, the strength of hydrophobic interactions is insufficient to compensate for the energetic loss of locating ethanol in an exclusively hydrophobic environment, resulting in a probability of locating ethanol in the bilayer center that is three orders of magnitude lower than locating ethanol at the lipid/water interface. The low cross-relaxation rates between terminal methyl protons of hydrocarbon chains and ethanol are as much the result of infrequent chain upturns as of brief excursions of ethanol into the region of lipid hydrocarbon chains near the glycerol. The combination of nuclear magnetic resonance measurements and molecular dynamics simulations offers a general pathway to study the interaction of small molecules with the lipid matrix at atomic resolution.

INTRODUCTION

The binding of ethanol molecules to the lipid matrix of biomembranes is an important, and still not well understood, event in anesthesia. For example, Mitchell and Litman (2000) recently reported that under physiologically relevant conditions, ~90% of the effect of ethanol on the G-protein coupled membrane receptor rhodopsin appears to be the result of changes in the acyl chain packing of the lipid matrix. In contrast, other work has emphasized the direct interaction of ethanol with membrane proteins (Mihic et al., 1997). Perhaps ethanol acts at multiple sites with variable emphasis on indirect interaction via the lipid matrix or direct interaction with the protein, depending on the specific protein system involved. Ultimately, approaches that resolve ethanol interaction with the constituents of biomembranes at atomic resolution are required to provide answers about the location of ethanol, the degree of immobilization of bound ethanol molecules, and the functional perturbation that ethanol causes in the lipid matrix and in proteins.

We have shown previously (Holte and Gawrisch, 1997) that the location of ethanol in the lipid matrix of biomembranes can be studied by two-dimensional magic angle spinning (MAS) nuclear Overhauser enhancement spectroscopy (NOESY). This method is sensitive to interactions on the angstrom length scale and to motions on the pico- to microsecond time scale, thus providing data with extremely high temporal and spatial resolution. Since our first paper appeared, the processes of spectral acquisition and data analysis have been greatly refined (Huster and Gawrisch, 1999; Huster et al., 1999; Yau and Gawrisch, 2000), and the possibility of comparison with molecular dynamics computer simulations has developed (Feller et al., 1999).

Recently, our laboratories have collaborated to use NOESY cross-relaxation rates in phospholipid bilayers as a tool for the validation of molecular dynamics (MD) simulations and to use simulation trajectories to understand the factors influencing these rates (Feller et al., 1999). In this paper we extend these methods to the important problem of solute partitioning into bilayer membranes. Details of the experimental and simulation methodologies are presented, followed by experimental and computational results that provide a picture of ethanol-membrane interactions in unprecedented detail. We conclude with a summary of the biological implications of these results and a discussion of possible extensions of these methods to other systems of biochemical interest.

Submitted June 29, 2001, and accepted for publication December 5, 2001.

Address reprint requests to Klaus Gawrisch, Laboratory of Membrane Biochemistry and Biophysics, NIAAA, National Institutes of Health, 12420 Parklawn Drive, Room 150, Rockville, MD 20852. Tel.: 301–594–3750; Fax: 301–594–0035; E-mail: gawrisch@helix.nih.gov.

0006-3495/02/03/1396/09 $2.00

MATERIALS AND METHODS

Sample preparation

The phospholipids 1-palmitoyl-2-oleoyl-*sn*-glycero-3-phosphocholine (POPC), 1-palmitoyl-2-oleoyl-*sn*-glycero-3-phosphocholine-*d4* (POPC-*d4*), and 1-palmitoyl-*d31*-2-oleoyl-*sn*-glycero-3-phosphocholine (POPC-

d31) were obtained from Avanti Polar Lipids (Alabaster, AL). Lipids were received as a powder and dried to a monohydrate in the presence of phosphorous pentoxide under a vacuum of 50 μm Hg for 24 h. Multilamellar vesicles were prepared by adding a mixture of ethanol in D_2O to ~50 mg of the dry lipid. The appropriate amount of ethanol solution was added to establish a molar ratio of lipid/ethanol/water of 1:1:10. The samples were sealed and subjected to centrifugation and temperature cycling between −20 and 50°C over 6 h to achieve homogeneity. Ten milligrams of sample were then transferred to an MAS insert and sealed inside a 4-mm rotor for magic angle spinning.

Nuclear magnetic resonance measurements

^{2}H Nuclear magnetic resonance (NMR) powder spectra were acquired on a Bruker DMX300 spectrometer at a resonance frequency of 46.1 MHz using a stationary dual resonance probe with a 4-mm solenoidal sample coil. Temperature was maintained at 10°C. A quadrupolar echo sequence (Davis et al., 1976) was used with two 1.8-μs 90° pulses and an interpulse delay of 50 μs. For the lipid resonances, 4096 scans with at a spectral width of 200 kHz and a delay time of 0.5 s were acquired. Deuterated ethanol and water required fewer scans. ^{2}H NMR powder pattern spectra were dePaked (Sternin et al., 1983; McCabe and Wassall, 1995) to give spectra that correspond to the 0° orientation of the bilayer normal with respect to the external magnetic field. Smoothed order parameter profiles of the palmitic chain of POPC were calculated according to Lafleur et al. (1989) and Holte et al. (1995).

NOESY NMR experiments with magic angle spinning were conducted on a Bruker DMX500 widebore spectrometer at a resonance frequency of 500.13 MHz. Sample spinning at 10 kHz was accomplished in a Bruker double gas bearing MAS probehead for 4-mm rotors. Compressed air was passed through a copper coil immersed in a cooling bath to maintain sample temperature at 10 ± 1°C. Temperature inside the spinning rotor was calibrated by recording the proton spectra of 1-stearoyl-2-oleoyl-*sn*-glyero-3-phosphocholine as a function of temperature to detect the gel-to-liquid crystalline phase transition at 6.6°C (Boggs and Tummler, 1993). Two-dimensional NOESY was carried out in the phase-sensitive mode. The pulse sequence ($90° - t_1 - 90° - \tau_m - 90°$ − acquire $[t_2])_n$ was used with 512 t_1 increments, mixing times, τ_m, from 5 to 800 ms, 2048 t_2, increments, and 16 scans per t_1-increment. A 3.7-μs 90° pulse and 3.3-kHz spectral width were used. The magnetic field strength was locked to the internal D_2O resonance of the sample, using the third channel of the MAS probe.

Intensity of diagonal- and cross-peaks was recorded as a function of mixing time and data were analyzed with XWIN-NMR software (Bruker Instruments, Billerica, MA). To more accurately measure volumes of cross-peaks between lipid and ethanol resonances, we performed signal deconvolution of the two-dimensional NOESY spectra using the curve fitting routine in SigmaPlot 5 (SPSS Inc., Chicago, IL). The resonances are reasonably well approximated by Gaussian peaks with peak position, peak width in *x*- and *y*-dimensions, and peak height as fitting parameters. Precision of the deconvolution procedure depends mostly on experimental artifacts, such as residual t_1-noise and deviation of line shapes from a Gaussian form, but also on the ratio of superimposed peak intensities. Typical experimental errors of fitted peak volumes are 10 to 20%. Cross-relaxation rates were calculated by a matrix algorithm that corrects for mild to moderate influences from spin diffusion and spin-lattice relaxation (Huster et al., 1999). No significant contributions from spin diffusion were detected for mixing times up to 400 ms.

Molecular dynamics simulations

The simulation protocol has been successfully applied to the simulation of numerous saturated and unsaturated phosphatidylcholine bilayers in the recent past (Feller et al., 1997a, 1999; Armen et al., 1998; Schneider and Feller, 2001) and is described here for completeness. The periodic simulation cell contained 72 lipids (36 per monolayer), 72 ethanol, and 720 water molecules, corresponding to the mole ratios of samples prepared for NMR investigations (see above). A partially flexible simulation cell was used with the *z* dimension (i.e., the bilayer normal) adjusted to maintain the $P_{zz} = 1$ atm, and the *x* and *y* dimensions fixed to maintain a surface area of 65 Å^2/molecule, as estimated from x-ray diffraction experiments on similar lipids (Koenig et al., 1997) after considering corrections from changes in *sn*-1 chain order due to differences in the level of hydration and the presence of ethanol. Initial coordinates for the POPC molecules were taken from a previously published POPC simulation (Armen et al., 1998).

The program CHARMM (chemistry at Harvard molecular mechanics) (Brooks et al., 1983) was used with the PARM22b4b all-atom parameter set (Schlenkrich et al., 1996; Feller and MacKerell, 2000) and its extension to unsaturated lipids (Feller et al., 1997b). The CHARMM potential contains internal energy terms for bond lengths, bond angles, torsional angles, and improper torsional angles. The interactions between nonbonded atoms are described by Coulombic interactions between partial point charges on the atomic centers and a Lennard-Jones 6-to-12 potential. The Lennard-Jones potential was switched smoothly to zero over the region from 10 to 12 Å. Electrostatic interactions were included via the particle mesh Ewald summation (Essmann and Berkowitz, 1999). All bonds involving hydrogen were fixed at their equilibrium distances using the SHAKE algorithm (Ryckaert et al., 1977). A time step of 2 fs was used with a modified leap-frog Verlet integration scheme. A neighbor list, used for calculating the Lennard-Jones potential and the real space portion of the Ewald sum, was kept to 14 Å and updated every 20 fs. A variant of the extended system formalism, the Langevin Piston algorithm (Feller et al., 1995), was used to control the normal pressure. The temperature was maintained at 10°C by means of the Hoover thermostat (Hoover, 1985). Coordinates sets were saved every 1 ps for subsequent analysis. Simulations were carried out using four or eight processors on a Beowulf-type parallel computer with each nanosecond of simulation taking ~5 days of wall time. The total simulation length was 11 ns. For data analysis, the first nanosecond of motions was discarded as equilibration time.

Calculation of NOESY cross-relaxation rates

The NOESY experiment probes the transfer of magnetization, occurring over a time interval referred to as the mixing time, from a set of magnetically equivalent protons (producing resonance *i*) to a second set (producing resonance *j*). The calculation of NOESY cross-relaxation rates from protein models and simulations has been described in the literature (Brüschweiler and Wright, 1994; Brüschweiler et al., 1992) and is briefly reviewed here. The connection between the experimental NOESY cross-relaxation rates and the molecular dynamics simulations is established through the magnetic dipolar interaction correlation function

$$C_{ij}(t) = \frac{4}{5}\sum_i\sum_j \left\langle \frac{Y_{20}(\vec{r}_{ij}(0))}{r_{ij}^3(0)} \frac{Y_{20}(\vec{r}_{ij}(t)}{r_{ij}^3(t)} \right\rangle, \qquad (1)$$

in which $Y_{20} = [5/16\pi]^{1/2}(3\cos^2\theta - 1)$, and θ is the angle between the internuclear vector, $\vec{r}_{ij}$, and the *z* axis (normal to the membrane). The summations over *i* and *j* include all magnetically equivalent protons of each resonance. From the MD simulation, the correlation function defined by Eq. 1 is calculated directly from the trajectory. It should be noted that the number of individual pair correlation functions is large, however, only those pairs with small internuclear separations contribute to the summation. Therefore, the finite size of the simulation cell does not affect the results. The cross-relaxation rates are calculated from the spectral density functions $J_{ij}(\omega)$, which are the Fourier transform of the correlation functions. Cross-relaxation rates depend on $J_{ij}(2\omega_0)$ and $J_{ij}(0)$ according to

$$\Gamma_{ij} = \zeta\,[3J_{ij}(2\omega_0) - \tfrac{1}{2}J_{ij}(0)] \qquad (2)$$

in which, ω_0 is the proton Larmor frequency, and $\zeta = (2\pi/5)\gamma^4\hbar^2(\mu_0/4\pi)^2$, in which γ is the gyromagnetic ratio for protons. The correlation function

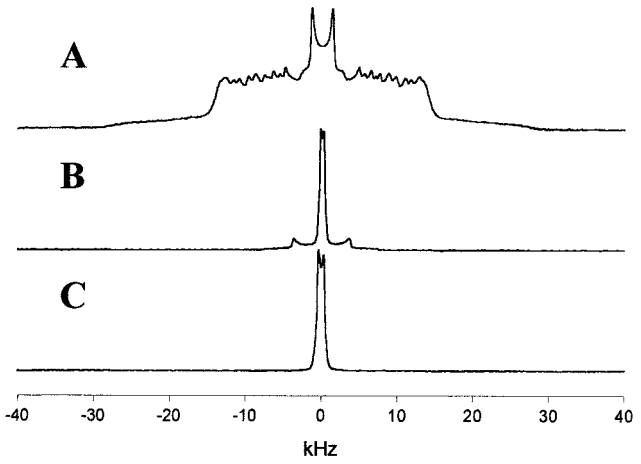

FIGURE 1 ^{2}H NMR spectra for POPC-*d31* (*A*), ethanol-*d5* (*B*), and D_2O (*C*) in POPC/ethanol/water (1:1:10, mol/mol) samples recorded at 10°C. (*A*) Superposition of quadrupole splittings of all *sn*-1 chain deuterons in POPC-*d31*; (*B*) superposition of the methylene and methyl group quadrupole splittings of ethanol; (*C*) single averaged quadruple splitting of all deuterons in water.

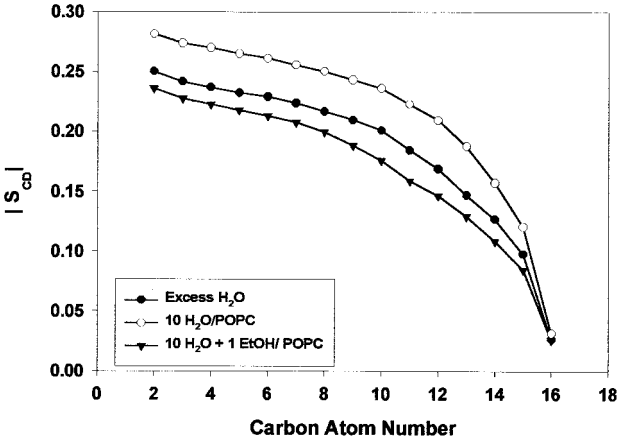

FIGURE 2 Influence of dehydration and ethanol on POPC *sn*-1 chain order parameter profiles recorded at 10°C. Dehydration of POPC bilayers from excess water to 10 waters per lipid increases chain order, whereas addition of one ethanol molecule per lipid decreases chain order.

defined by Eq. 1 was calculated from the methylene protons of each ethanol to each of the unique ^1H lipid resonances observed experimentally. The raw correlation functions were fit to a sum of four exponentials as described previously (Feller et al., 1999), $C(t) = \Sigma_{i=1}^{4} a_i e^{-1/\tau_i}$, allowing the Fourier transform to be performed analytically and the contribution from each exponential to the overall cross-relaxation rate to be quantified.

When interpreting the Γ_{ij} it is important to emphasize that these cross-relaxation rates are determined both by structural considerations (the probability of close contact between protons) and dynamic factors (the relaxation of the proton-proton internuclear vector). The MD simulation results, by providing a direct picture of the underlying correlation function, $C_{ij}(t)$, can be used to quantify these contributions. The probability of close contact is measured by the magnitude of $C_{ij}(0)$, which is proportional to $\langle 1/r_{ij}^6 \rangle$ and thus extremely sensitive to the number of very close contacts. In terms of the fit parameters, this quantity is given by the sum of the intensity factors, a_i, and will be denoted a_s. The dependence of Γ_{ij} on relaxation time is seen most easily by considering a simple single exponential decay of the correlation function:

$$C(t) = C(0)e^{-t/\tau} \rightarrow J(\omega)$$

$$= \frac{2C(0)\tau}{1 + \tau^2\omega^2} \rightarrow \Gamma = C(0)\zeta\left[\frac{6\tau}{1 + 4\tau^2\omega_0^2} - \tau\right] \quad (3)$$

Due to the difference in sign between the contributions of $J_{ij}(2\omega_0)$ and $J_{ij}(0)$ to Γ_{ij} (see Eq. 2), correlation times, τ, longer than ~400 ps lead to negative cross-relaxation rates for a proton Larmor frequency of 500 MHz.

RESULTS AND DISCUSSION

Characterization of the state of POPC, ethanol, and water by ^{2}H NMR

As visible from the deuterium spectra and chain order parameter profiles (Figs. 1 and 2), POPC is in the lamellar state. The effects of dehydration and ethanol addition on chain order have opposite sign and similar magnitude. Dehydration from excess water to 10 waters per lipid increased chain order parameters, whereas addition of one ethanol per lipid lowered them (Fig. 2). Both ethanol and water interact with the lipid, leading to anisotropic solvent motions and quadrupolar interactions of the ^{2}H nuclei with the electric field gradients within these molecules that only partially average out. The order parameters of the ethanol C—D_2 bonds, ethanol C—D_3 bonds, and water O—D bonds, are 0.064, 0.004, and 0.005, respectively. Such values are characteristic for temporary association of solvent molecules with the lipid/water interface (Barry and Gawrisch, 1994; Gawrisch et al., 1992). The MD simulation gave similarly low values for the order parameters of 0.039, 0.010, and 0.008 with standard deviations of ~0.020.

^{1}H MAS NOESY NMR

The resolution of resonance lines allows detection of 13 proton signals, 10 from POPC, two from ethanol, and one from water (Fig. 3). Improvements in the design of MAS rotor inserts and MAS probeheads resulted in two-dimensional NOESY spectra (Fig. 4) with lower t_1-noise compared with our previous investigation (Holte and Gawrisch, 1997). Resonance signals of ethanol are partially superimposed on lipid resonances. To reduce the influence from signal superposition on cross-peak intensities, we also studied POPC-*d4* with two deuterated methylene groups in the choline headgroup, and POPC-*d31* with a perdeuterated *sn*-1 palmitic acid chain. The chain-deuterated lipid only reduced signal superposition, whereas the headgroup deuterated POPC allowed unperturbed observation of ethanol-CH_2 cross-relaxation with lipid resonances. Intensities of partially superimposed cross-peaks were determined by deconvolution as described under Materials and Methods.

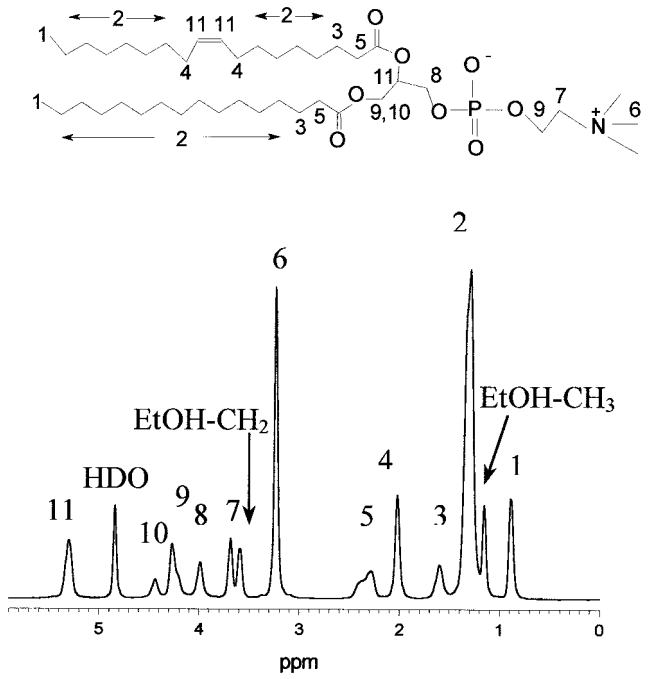

FIGURE 3 The 500-MHz magic-angle spinning ^{1}H NMR spectrum of a POPC/ethanol/D_2O sample (1:1:10, mol/mol) with peak assignments, recorded at a spinning speed of 10 kHz and a temperature of 10°C.

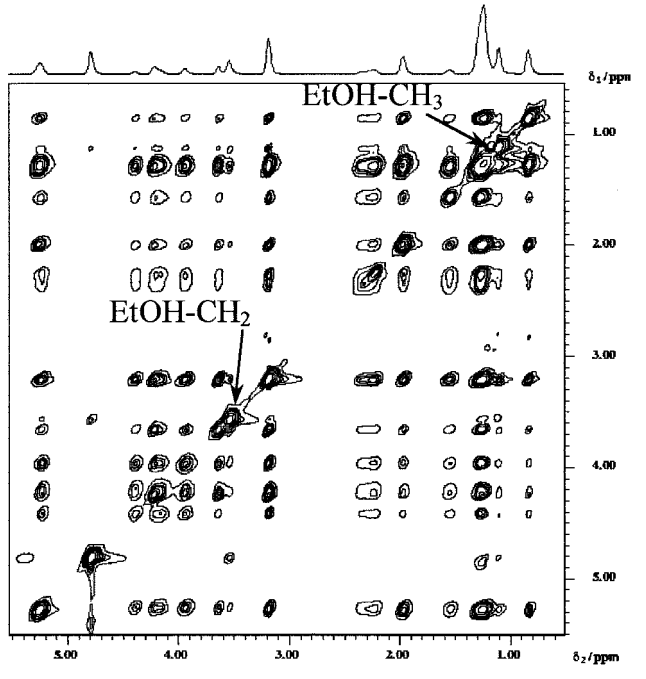

FIGURE 4 Two-dimensional NOESY contour plot of the sample shown in Fig. 3, recorded at a mixing time of 400 ms. Sets of cross-peaks between ethanol and lipid resonances have been detected. The cross-peak volume as a function of mixing time was determined by integration. Two-dimensional deconvolution procedures were applied to determine cross-peak volumes of partially superimposed resonances.

Fig. 5 gives the per-proton cross-relaxation rates between ethanol and lipid resonances. Measured cross-relaxation rates are highest for interaction of ethanol with interface lipid protons, particularly with those in the glycerol region. There is an intriguing difference in cross-relaxation rates between ethanol-methyl and ethanol-methylene groups. Whereas methyl groups have stronger cross-relaxation with chain signals, methylene groups interact more strongly with headgroup resonances, suggesting that the ethanol molecule is oriented with its methyl group toward the hydrophobic bilayer core. Additional evidence for this orientation comes from the MD simulation. We found that the orientation of ethanol is such that the average distance of the methyl group to the bilayer center is 0.65 Å less than the distance to the hydroxyl oxygen.

Cross-relaxation rates from MD simulations

Fig. 6 shows examples of correlation functions calculated from the MD trajectory. Correlation functions were fit to a sum of four superimposed exponentials as described in Materials and Methods. Fit parameters are reported in Table 1. Based on previous analysis of the time scales of lipid dynamics (Pastor and Feller, 1996), the four relaxation rates can be attributed to various motions in the lipid matrix. Librational motions of ethanol and lipid chemical bonds cause the very fast initial decay of correlation functions with correlation times of a few picoseconds. The decay with correlation times in the range of 100 ps is the result of gauche-trans isomerization, correlation times from 500 to 1000 ps are caused by molecular rotation and wobble, and

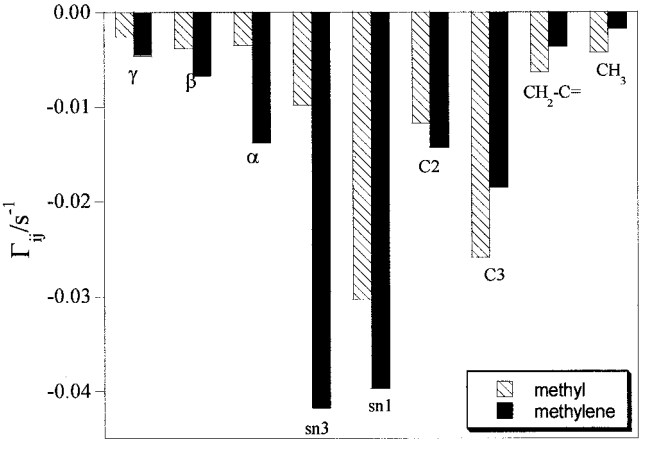

FIGURE 5 Experimental lipid-ethanol per-proton cross-relaxation rates as a function of position along the membrane normal. Filled and unfilled bars give the methyl and methylene results, respectively. The abbreviations α, β, γ indicate choline methylene, and methyl groups, *sn*-1 and *sn*-3, are the corresponding glycerol methylene groups, C_2 and C_3 are the chain methylene groups near the glycerol, CH_2—C = the two methylene groups near the double bond in the *sn*-2 chain, and CH_3 the terminal methyl groups of palmitic- and oleic acid chains.

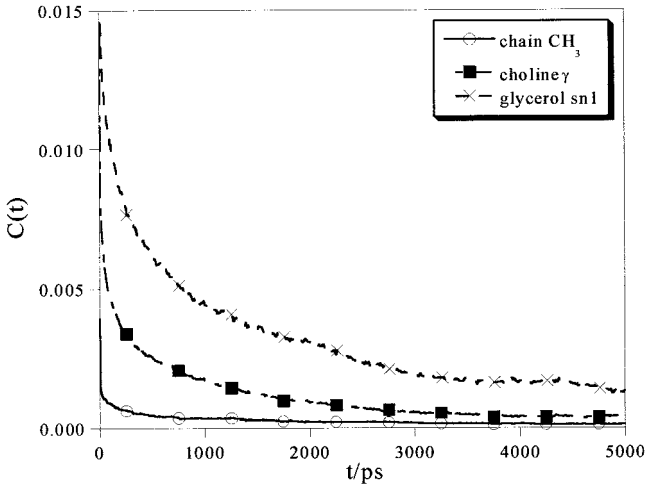

FIGURE 6 Dipolar correlation function for interactions between the ethanol methylene group with choline methyl-, glycerol *sn*-1-, and chain methyl groups. Correlation functions can be approximated by a superposition of four exponentials with correlation times corresponding to librational motions of ethanol and lipid chemical bonds (≈5 ps), gauche-trans isomerization (≈100 ps), molecular rotation and wobble (500–1000 ps), and the diffusive motions of the smaller ethanol molecules within the lipid matrix (3–11 ns).

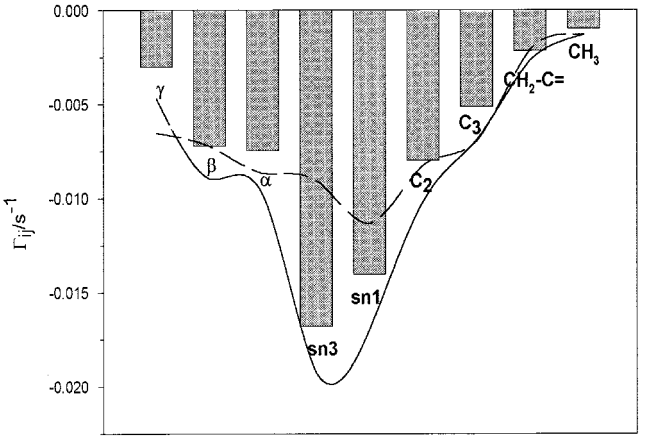

FIGURE 7 Calculated lipid-ethanol per-proton cross-relaxation rates as a function of position along the membrane normal. The bars represent the rates, Γ_{ij}, as calculated by Eq. 4. The solid line represents the contribution from the spectral density function $J_{ij}(0)$ to Γ_{ij}. The dashed line is a scaled presentation of the intensity of correlation functions at time 0, $C(0)$ (equivalent to a_s in Table 1). Cross-relaxation rates are dominated by contributions from spectral density function $J_{ij}(0)$.

finally, correlation times in the multinanosecond range are related to the diffusive motions of the smaller ethanol molecules within the lipid matrix.

Table 1 also provides the experimental and simulation results for the cross-relaxation rates between ethanol methylene protons and each resolved peak in the POPC spectrum. Both experiment and simulation give the same trend of rates of magnetization transfer between ethanol and lipid hydrocarbon-, glycerol-, and headgroup resonances (compare Fig. 5 and 7), i.e., the strongest magnetization transfer occurs to lipid resonances at or near the lipid/water interface, including upper segments of lipid hydrocarbon chains, glycerol, and lipid headgroups. Cross-relaxation rates decrease both going into the choline segments and moving further down the lipid chains to the center of the hydrophobic core. Considering the high sensitivity of cross-relaxation rates to experimental conditions such as temperature and water content, comparison of measured and calculated rates resulted in very good agreement.

Dynamic factors influencing the magnitude of NOESY cross-relaxation rates

We have calculated the contributions to the cross-relaxation rates from the spectral density functions $J_{ij}(0)$ and $J_{ij}(2\omega_0)$. Results are summarized in Fig. 7. The spectral contributions $J_{ij}(0)$ from motions with the correlation time, τ_4, and the amplitude, a_4, (diffusive motions of ethanol molecules within the lipid/water interface) are dominating the cross-relaxation rates with their large negative values. The fast motions with correlation times of less than 400 ps contribute to $J_{ij}(2\omega_0)$ and result in a small positive correction to the overall negative cross-relaxation rates. At 10°C the correction is of the order of 5 to 20% (the bars in Fig. 7 represent the total cross-relaxation rates Γ_{ij}, the solid line is the $J_{ij}(0)$-contribution only). Nonetheless, the ethanol/lipid

TABLE 1 Parameters describing the ethanol methylene-lipid dipolar correlation function as calculated from the MD simulation

Lipid group	a_1	τ_1/ps	a_2	τ_2/ps	a_3	τ_3/ps	a_4	τ_4/ps	a_s	τ_{ave}/ps	Γ^{sim}/s^{-1}	Γ^{exp}/s^{-1}
Choline γ	0.0120	4.8	0.00362	88.7	0.00248	753.0	0.00149	2921.5	0.0196	336.7	−0.0030	−0.0047
Choline β	0.0119	4.3	0.00405	66.8	0.00442	918.8	0.00131	6206.0	0.0217	577.5	−0.0072	−0.0067
Choline α	0.0141	3.9	0.00460	69.2	0.00367	426.9	0.00362	3237.7	0.0260	524.8	−0.0074	−0.0138
Glycerol *sn*-3	0.0148	4.8	0.00432	114.4	0.00611	862.6	0.00185	11380.2	0.0270	996.6	−0.0168	−0.0418
Glycerol *sn*-1	0.0204	5.0	0.00558	153.6	0.00527	1146.1	0.00274	6070.5	0.0340	694.1	−0.0140	−0.0397
Chain C2	0.0148	4.9	0.00363	126.3	0.00370	669.3	0.00252	4431.8	0.0247	573.8	−0.0080	−0.0143
Chain C3	0.0126	4.5	0.00293	99.8	0.00344	611.6	0.00189	3790.0	0.0209	460.7	−0.0051	−0.0185
CH_2—C═C	0.0037	4.3	0.00085	96.5	0.00056	482.5	0.00115	2893.7	0.0063	586.3	−0.0022	−0.0036
Chain CH_3	0.0027	4.6	0.00067	173.7	0.00012	557.8	0.00044	3649.2	0.0039	454.0	−0.0010	−0.0017

cross-relaxation rates are such that they are sensitive to the competing contributions of $J_{ij}(0)$ and $J_{if}(2\omega_0)$. Not only does $J_{ij}(0)$ decline with increasing temperature because τ_4 becomes smaller, but the contribution from $J_{if}(2\omega_0)$ (with opposite sign) simultaneously increases. We propose that this explains the tremendous sensitivity of measured cross-relaxation rates to temperature and water content of samples.

Fig. 7 also shows the importance of taking into account differences in relaxation rates between the correlation functions for each lipid segment. The scaled intensity of the correlation function at time 0, $C(0)$ (dashed line in Fig. 7), poorly predicts differences between cross-relaxation rates, demonstrating that dynamic factors play an important role in the relative cross-relaxation rates. Differences in the longest correlation time, τ_4, have the most significant influence on these rates. This correlation time represents an effective lifetime of temporary associations between lipid and ethanol. The lifetime of these associations with functional groups at the hydrophobic/hydrophillic interface is increased compared with those that occur in the aqueous layer (Table 1).

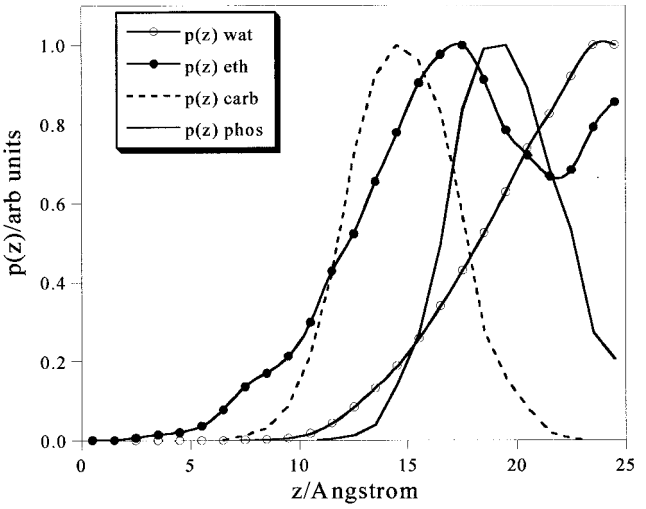

FIGURE 8 Probability distribution for ethanol and water as a function of position within the membrane. The location of the phosphate and carbonyl groups are shown for reference. Ethanol density has a local maximum near the location of lipid phosphate groups. Ethanol penetrates deeper into the lipid/water interface region compared with water molecules.

Location of ethanol molecules in the lipid bilayer

The significant difference in ethanol-lipid cross-relaxation rates (Fig. 5), and in the magnitude of the choline and glycerol correlation functions (Fig. 6), suggests that the density of ethanol in the vicinity of the glyercol segment is higher than near the choline. To address the relationship between local ethanol density and NOESY cross-relaxation rates, the concentration of ethanol through the lipid bilayer, derived from the MD simulation, has been plotted in Fig. 8. Ethanol prefers the aqueous phase and the lipid water interface but can also penetrate into the lipid bilayer to the region of upper chain segments. Notice that the location of highest ethanol density is between the carbonyl and phosphate groups, i.e., coincident with the glycerol segment that is found, from both experiment and simulation, to have the highest rates of cross-relaxation. Due to its partial hydrophobicity, penetration into the hydrophobic regions of the bilayer is significantly deeper compared with water. The relatively low energetic cost of ethanol penetration into the interface region is quantified by the potential of mean force calculations presented in Fig. 9. Ethanol-free energy near the lipid phosphate groups is the same as in water but increases exponentially with decreasing distance from the bilayer center. Locating ethanol or water in the center of the hydrophobic core ($z = 0$) is energetically very unfavorable with the probability of finding an ethanol molecule in the bilayer center ~1000 times lower than finding ethanol in the water phase.

In Figs. 5, 6, and 8, we have demonstrated that the highest NOESY cross-relaxation rates correspond to those segments of the lipid molecule that reside in the region of highest ethanol density. The origin of this high ethanol density near $z = 17.5$ Å is the strong interaction between ethanol and the lipid phosphate and carbonyl groups. This is shown clearly in Fig. 10 where the lipid-ethanol interaction energies from the MD simulation have been decomposed into contributions from submolecular fragments of the lipid molecule. The strongest ethanol interactions are observed with the phosphate and carbonyl groups, thus placing the ethanol methyl and methylene protons in close proximity to lipid

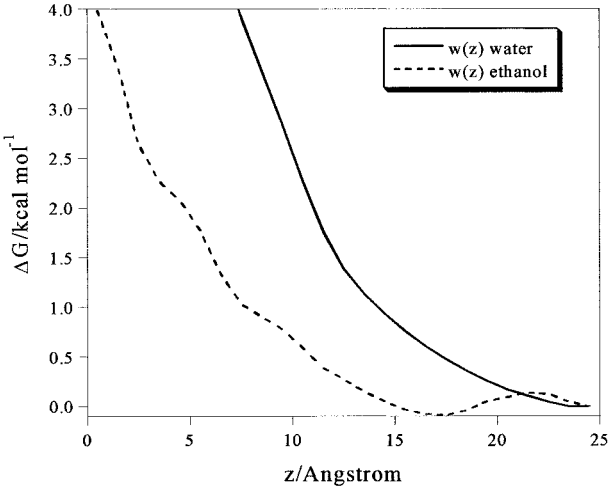

FIGURE 9 Potential of mean force for water (*solid line*) and ethanol (*dashed line*) as a function of position along the bilayer normal. The increase of ethanol-free energy by 4 kcal/mol corresponds to an ~1000-fold lower probability of finding ethanol in the bilayer center compared with the water phase or the lipid/water interface region near the phosphate groups.

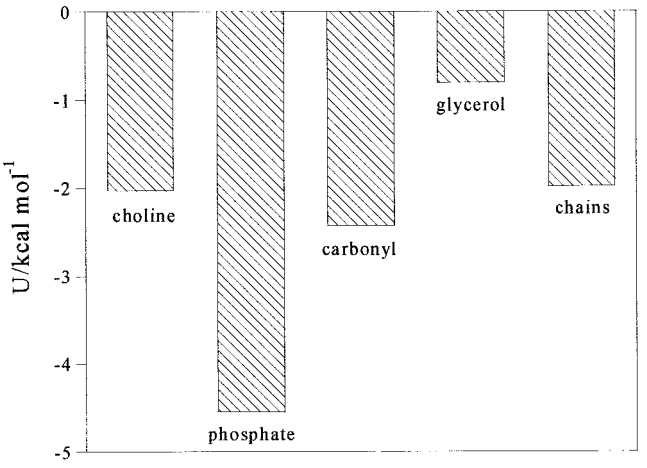

FIGURE 10 Average interaction energy between ethanol molecules and the various submolecular fragments of POPC. Attractive interaction is strongest with lipid phosphate groups, followed by hydrocarbon chain carbonyls, choline groups, hydrocarbon chains, and glycerol. The strong interaction with phosphate groups is the result of formation of hydrogen bonds.

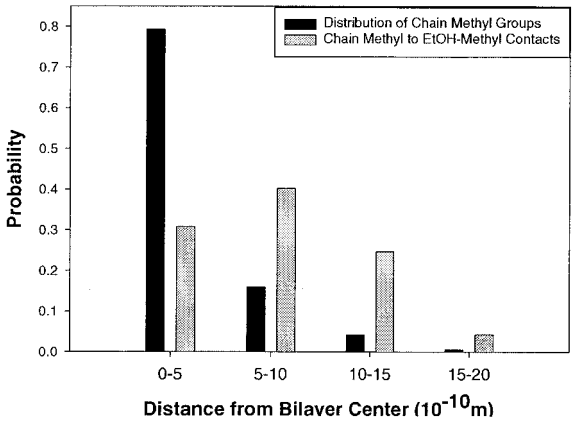

FIGURE 12 Probabilities of chain methyl location (*black bars*) and ethanol-chain methyl contacts defined as approach to a distance of 6 Å or less (*gray bars*) as a function of distance from bilayer center. Intensities were averaged over slabs with a thickness of 5 Å. The probability of contacts between ethanol and chain methyl groups is highest in the hydrocarbon chain region near the interface, indicating infrequent chain upturns and brief excursions of ethanol molecules into regions of upper chain segments.

protons of the glycerol and upper chain segments of the molecule and causing the high rates of cross-relaxation. A typical lipid/ethanol conformation is displayed in Fig. 11,

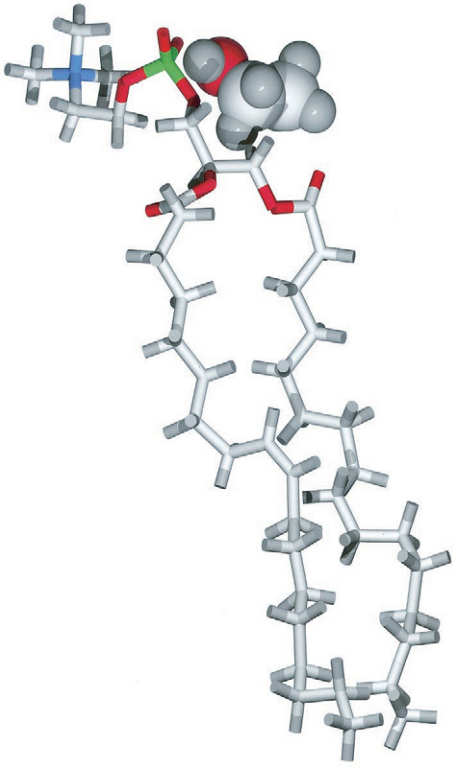

FIGURE 11 Representative conformation of a temporary association of ethanol with a phospholipid molecule. Ethanol prefers to form hydrogen bonds with the lipid phosphate group whereas the ethyl residue is directed toward the bilayer hydrophobic core.

showing a hydrogen bond between the polar ethanol hydrogen and a phosphate oxygen. The strong interactions between ethanol and lipid groups further modulate the observed cross-relaxation rates by increasing the lifetime of ethanol-lipid contacts. This is seen in Table 1 where the correlation functions for the glycerol segments have the longest mean relaxation times of any segments. Additionally, the dipolar correlation function depends not on r_{ij}, i.e., the simple distance between protons, but is instead a function of r_{ij}^6. Thus, a small number of close contacts with long residence times can outweigh more frequent contacts at longer distances and/or shorter duration.

It should be emphasized that, due to the inherent disorder of lipids within the bilayer, ethanol-lipid contacts do not necessarily occur at the average location of the lipid segments. For example, there is a small but measurable cross-relaxation between the ethanol methyl group and the terminal methyl group of hydrocarbon chains. According to Fig. 8, the probability of ethanol penetration into the membranes hydrophobic core is extremely low. This raises the question of where ethanol and hydrocarbon chain methyl groups meet. We divided the simulated membrane into slabs of 5 Å thickness and estimated the spatial origin of magnetization transfer between these methyl protons (Fig. 12). The black bars represent the distribution of chain methyl groups, whereas the gray bars are the distribution of contacts between chain and ethanol methyl groups, defined as approach to a distance of 6 Å or less. Probability of contact between ethanol and lipid methyl groups is highest in the hydrocarbon chain region near the lipid/water interface and in the interface region. Therefore the contacts between methyl groups of ethanol and lipid hydrocarbon chains are both a reflection of lipid hydrocarbon chain upturns and excursions

of ethanol molecules into the upper hydrophobic chain region of membranes.

Concluding remarks

The quantitative analysis of two-dimensional NOESY spectra from lipid membranes has greatly increased the number of NMR parameters of membranes. For example, the total number of order- and relaxation parameters that were measured for the ethanol-POPC samples exceeds 100. In contrast to NOESY cross-relaxation rates in proteins, cross-relaxation in the lipid matrix does not report a fixed geometry of biomolecules, but reflects the distribution function of lipid- and solvent segments along the bilayer normal, the probability of short-lived associations, and the presence of motions within membranes covering correlation times in the range from pico- to microseconds. The good agreement between simulation and experiment serves to validate the model and computational protocol. Furthermore, the NMR parameters reflect intricate details on membrane structure, dynamics, and solvent interactions that can be interpreted quantitatively when the experiments are combined with MD simulations. Thus, the present study lays a foundation for further studies of membrane solute interactions via NOESY spectroscopy and MD simulation.

The combination of spectroscopic and simulation results unambiguously places ethanol at the membrane/water interface, specifically in the chemically heterogeneous region between the phosphate and carbonyl groups. Ethanol interacts with the lipid matrix primarily via hydrophilic interactions like hydrogen bonds and gains only modestly from hydrophobic interactions with upper chain segments. Although an interface location of ethanol was predicted previously on the basis of Fourier transform infrared (Chiou et al., 1990; Klemm, 1990), NMR (Holte and Gawrisch, 1997; Barry and Gawrisch, 1994, 1995; Klemm and Williams, 1996), and fluorescence studies (Slater et al., 1993), the current experiments excel in temporal and spatial resolution of ethanol membrane interaction. Ethanol molecules prefer the lipid/water interface but can penetrate into the region of upper chain segments. This location is primarily facilitated by hydrogen bonding between ethanol and the lipid phosphate groups, but also by hydrogen bonding to carbonyls and by weak hydrophobic van der Waals attraction between the short ethyl group and upper chain segments. The hydrophobic contributions to this interaction are unable to compete with the strong desire of ethanol to form hydrogen bonds, thus preventing high concentrations of ethanol within the hydrophobic core.

We speculate that interaction of ethanol with the interface region of proteins is governed by similar needs to satisfy hydrophilic interactions, aided by small gains from inserting the ethyl groups into a hydrophobic environment. We expect that ethanol interacts with the same functional groups on protein surfaces as in the lipid/water interface region. Interestingly, phosphorylation of proteins is a common mechanism to control activity. Perhaps, ethanol binding to phosphorylation sites of proteins is one of the mechanisms by which ethanol influences protein function.

S. E. Feller and C. A. Brown were supported by grant MCB-0091508 from the National Science Foundation.

REFERENCES

Armen, R. S., O. D. Uitto, and S. E. Feller. 1998. Phospholipid component volumes: determination and application to bilayer structure calculations. *Biophys. J.* 75:734–744.

Barry, J. A., and K. Gawrisch. 1994. Direct NMR evidence for ethanol binding to the lipid-water interface of phospholipid bilayers. *Biochemistry.* 33:8082–8088.

Barry, J. A., and K. Gawrisch. 1995. Effects of ethanol on lipid bilayers containing cholesterol, gangliosides, and sphingomyelin. *Biochemistry.* 34:8852–8860.

Boggs, J. M., and B. Tummler. 1993. Interdigitated gel phase bilayers formed by unsaturated synthetic and bacterial glycerophospholipids in the presence of polymyxin-B and glycerol. *Biochim. Biophys. Acta.* 1145:42–50.

Brooks, B. R., R. E. Bruccoleri, B. D. Olafson, D. J. States, S. Swaminathan, and M. Karplus. 1983. CHARMM: a program for macromolecular energy, minimization, and dynamics calculations. *J. Comp. Chem.* 4:187–217.

Brüschweiler, R., B. Roux, M. Blackenledge, C. Griesinger, M. Karplus, and R. R. Ernst. 1992. Influence of rapid intramolecular motion on NMR cross-reaxation rates: a molecular-dynamics study of antamanide in solution. *J. Am. Chem. Soc.* 114:2289–2302.

Brüschweiler, R., and P. E. Wright. 1994. Water self-diffusion model for protein-water NMR cross-relaxation. *Chem. Phys. Lett.* 229:75–81.

Chiou, J. S., S. M. Ma, H. Kamaya, and I. Ueda. 1990. Anesthesia cutoff phenomenon: interfacial hydrogen-bonding. *Science.* 248:583–585.

Davis, J. H., K. R. Jeffrey, M. Bloom, M. I. Valic, and T. P. Higgs. 1976. Quadrupolar echo deuteron magnetic resonance spectroscopy in ordered hydrocarbon chains. *Chem. Phys. Lett.* 42:390–394.

Essmann, U., and M. L. Berkowitz. 1999. Dynamical properties of phospholipid bilayers from computer simulation. *Biophys. J.* 76:2081–2089.

Feller, S. E., D. Huster, and K. Gawrisch. 1999. Interpretation of NOESY cross-relaxation rates from molecular dynamics simulation of a lipid bilayer. *J. Am. Chem. Soc.* 121:8963–8964.

Feller, S. E., and A. D. MacKerell. 2000. An improved empirical potential energy function for molecular simulations of phospholipids. *J. Phys. Chem. B.* 104:7510–7515.

Feller, S. E., R. M. Venable, and R. W. Pastor. 1997a. Computer simulation of a DPPC phospholipid bilayer: structural changes as a function of molecular surface area. *Langmuir.* 13:6555–6561.

Feller, S. E., D. X. Yin, R. W. Pastor, and A. D. MacKerell. 1997b. Molecular-dynamics simulation of unsaturated lipid bilayers at low hydration: parametrization and comparison with diffraction studies. *Biophys. J.* 73:2269–2279.

Feller, S. E., Y. H. Zhang, R. W. Pastor, and B. R. Brooks. 1995. Constant-pressure molecular-dynamics simulation: the Langevin piston method. *J. Chem. Phys.* 103:4613–4621.

Gawrisch, K., D. Ruston, J. Zimmerberg, V. A. Parsegian, R. P. Rand, and N. Fuller. 1992. Membrane dipole potentials, hydration forces, and the ordering of water at membrane surfaces. *Biophys. J.* 61:1213–1223.

Holte, L. L., and K. Gawrisch. 1997. Determining ethanol distribution in phospholipid multilayers with MAS-NOESY spectra. *Biochemistry.* 36: 4669–4674.

Holte, L. L., S. A. Peter, T. M. Sinnwell, and K. Gawrisch. 1995. ^{2}H nuclear magnetic resonance order parameter profiles suggest a change of

molecular shape for phosphatidylcholines containing a polyunsaturated acyl chain. *Biophys. J.* 68:2396–2403.

Hoover, W. G. 1985. Canonical dynamics: equilibrium phase-space distributions. *Phys. Rev. A.* 31:1695–1697.

Huster, D., K. Arnold, and K. Gawrisch. 1999. Investigation of lipid organization in biological membranes by two-dimensional nuclear overhauser enhancement spectroscopy. *J. Phys. Chem. B.* 103:243–251.

Huster, D., and K. Gawrisch. 1999. NOESY NMR crosspeaks between lipid headgroups and hydrocarbon chains: spin diffusion or molecular disorder? *J. Am. Chem. Soc.* 121:1992–1993.

Klemm, W. R. 1990. Dehydration: a new alcohol theory. *Alcohol.* 7:49–59.

Klemm, W. R., and H. J. Williams. 1996. Amphiphilic binding site of ethanol in reversed lipid micelles. *Alcohol.* 13:133–138.

Koenig, B. W., H. H. Strey, and K. Gawrisch. 1997. Membrane lateral compressibility determined by NMR and X-ray diffraction: effect of acyl chain polyunsaturation. *Biophys. J.* 73:1954–1966.

Lafleur, M., B. Fine, E. Sternin, P. R. Cullis, and M. Bloom. 1989. Smoothed orientational order profile of lipid bilayers by ^{2}H nuclear magnetic resonance. *Biophys. J.* 56:1037–1041.

McCabe, M. A., and S. R. Wassall. 1995. Fast-fourier-transform dePaking. *J. Magn. Reson. B.* 106:80–82.

Mihic, S. J., Q. Ye, M. J. Wick, V. V. Koltchine, M. A. Krasowski, S. E. Finn, M. P. Mascia, C. F. Valenzuela, K. K. Hanson, E. P. Greenblatt, R. A. Harris, and N. L. Harrison. 1997. Sites of alcohol and volatile anaesthetic action on GABA(A) and glycine receptors. *Nature.* 389: 385–389.

Mitchell, D. C., and B. J. Litman. 2000. Effect of ethanol and osmotic stress on receptor conformation: reduced water activity amplifies the effect of ethanol on metarhodopsin II formation. *J. Biol. Chem.* 275: 5355–5360.

Pastor, R. W., and S. E. Feller. 1996. Time scales of lipid dynamics and molecular dynamics. *In* Biological Membranes: A Molecular Perspective from Computation and Experiment. K.M. Merz and B. Roux, editors. Birkhauser, Boston. 3–30.

Ryckaert, J. P., G. Ciccotti, and H. J. C. Berendsen. 1977. *J. Comp. Phys.* 23:327–341.

Schlenkrich, M., J. Brickmann, A. D. MacKerell, and M. Karplus. 1996. Biological Membranes: A Molecular Perspective from Computation and Experiment. Birkhäuser, Boston. 31–81.

Schneider, M. J., and S. E. Feller. 2001. Molecular dynamics simulations of a phospholipid-detergent mixture. *J. Phys. Chem. B.* 105:1331–1337.

Slater, S. J., C. Ho, F. J. Taddeo, M. B. Kelly, and C. D. Stubbs. 1993. Contribution of hydrogen-bonding to lipid lipid interactions in membranes and the role of lipid order: effects of cholesterol, increased phospholipid unsaturation, and ethanol. *Biochemistry.* 32:3714–3721.

Sternin, E., M. Bloom, and A. L. MacKay. 1983. De-pake-ing of NMR spectra. *J. Magn. Reson.* 55:274–282.

Yau, W. M., and K. Gawrisch. 2000. Lateral lipid diffusion dominates NOESY cross-relaxation in membranes. *J. Am. Chem. Soc.* 122: 3971–3972.